Cathodic protection with localised galvanic anodes in slender carbonated concrete elements

Elena Redaelli*, Federica Lollini, Luca Bertolini

Politecnico di Milano, Department of Chemistry, Materials and Chemical Engineering "Giulio Natta" – Piazza Leonardo da Vinci 32 – 20133 Milano (Italy)

* corresponding author: Elena Redaelli

Tel. +39 02 2399 3115

Fax +39 02 2399 3180

E-mail elena.redaelli@polimi.it

Abstract: A combined experimental and numerical investigation was carried out with the aim of determining whether few localised galvanic anodes per unit length could protect the reinforcement of slender carbonated concrete elements, exposed to atmospheric conditions, which could not be repaired with traditional methods. Initially, the cathodic behaviour of steel under galvanostatic polarisation was determined on small-size specimens obtained from a real element. A correlation of potential versus applied current was obtained. The current distribution in slender elements was then determined through finite elements simulations, considering various scenarios of carbonation and humidity. Results showed that, in spite of the high electrical resistivity of carbonated concrete, anodes with spacing of 0.45 m are enough to protect corroding reinforcement in most exposure conditions, even in thin parts of element. Estimated anode durations were of the order of several years or even decades; however, it was shown that also reinforcement in dry (carbonated or alkaline) concrete, which does not need to be protected, contributes to anode consumption. Although other aspects play a role on the performance of a cathodic protection system (such as the effectiveness of anode-encasing material and of electrical connection to reinforcement), the results obtained are supportive of a repair strategy based on the use of localised galvanic anodes and can be generalised to slender elements exposed to atmospheric conditions suffering carbonation induced corrosion.

Keywords (4-6): Carbonation, Cathodic protection, Concrete, Current distribution, Galvanic anode, Localised anode.

1 Introduction

The selection of the repair method for concrete structures damaged by carbonation-induced corrosion of reinforcement is a challenging task in those cases where the need to preserve the original surface, shape and materials makes a conventional intervention impossible or unacceptable. This is the case, for instance, of buildings and monuments of modern architecture, for which issues related to conservation are often of primary importance (as well as those related to safety or costs) in the selection of the repair method (Heinemann et al. 2008; Macdonald 2003; Matthews 2007). In other circumstances, the need to limit the alteration of the structure stems from the necessity to reduce the invasiveness of the intervention, for instance to keep the building in service during the repair operations or to reduce the generation of noise, dust and waste materials connected with concrete removal.

To this regard, electrochemical techniques may be a valid alternative compared to conventional repair because they allow to preserve non-protective carbonated concrete, provided it is not damaged (cracked or spalled) by reinforcement corrosion yet (Schiessl 1994). Amongst these, cathodic protection (*CP*), that in the past was mainly used for chloride-contaminated concrete, is nowadays an option even for carbonation-induced corrosion thanks to advantages connected with the possibility of leaving carbonated concrete in place and, so, minimising its replacement (Pedeferri 1996; Lambert 1995; Bertolini et al. 1998; Polder 1998; Sitton et al. 1998).

Further advantages in terms of reduced invasiveness of the intervention may be achieved if small localised anodes could be used instead of traditional surface-distributed anode systems (Bennet et al. 2008). In particular, localised galvanic anodes, that could be simply connected to the steel reinforcement (ideally without the need of electrical cabling), allow minimising the repair operations and avoid or limit the subsequent permanent monitoring system required by impressed current *CP*. Such anodes could be shaped as small cylinders to be inserted inside concrete or stripes to be placed on the concrete surface. Galvanic anodes have to be in contact with a proper electrolyte that prevents metal passivation and allows current circulation (Jordan and Page 2003). They do not require an external current generator and, unlike inert anodes used in impressed current systems, accidental contact with steel reinforcement does not impair the functioning of the

CP system. Galvanic anodes are self-regulating since the current they supply is determined by the electrochemical condition of steel and anode material (the latter is usually zinc activated by a proper embodying material) and by the electrical resistivity of concrete; both may change in time as a consequence of variations in humidity, carbonation, etc. (Redaelli et al. 2011; Holmes et al. 2011). Advantages connected with the use of localised anodes, however, may be partially compensated by their intrinsic limitation related to current distribution. In elements subject to carbonation, current distribution issues may be particularly critical due to increased electrical resistivity of carbonated concrete compared to alkaline concrete (Polder et al. 2000).

The study that will be presented in this paper started from the need to define a method for the repair of the reinforced concrete newels on the facades of a building exposed to urban environment (Bertolini et al. 2009). The elements are characterised by a slender, rather complex shape, as shown in Figure 1, and their function is mainly decorative. Almost 2000 elements are present on the facades of the building; they are not identical due to slight differences in geometry. After 50 years since the construction, some elements show the presence of cracks and local spalls of concrete cover. A preliminary condition evaluation revealed that damage is due to carbonation-induced corrosion of reinforcement; many elements are expected to be in a condition of high risk of falling of concrete debris, which is unacceptable for safety reasons. The repair method is required to maximise the preservation of the original material, shape and surface of elements and, at the same time, to fulfil adequate durability due to the difficulty in accessing the facades for future maintenance. *CP* with localised galvanic anodes is considered as a possible repair option and a preliminary design of the *CP* system is required, including an estimation of the number of anodes that is necessary to protect the reinforcement. To this purpose, the current distribution needs to be evaluated, and this has been done through different approaches.

Initially, the potential distribution that could be achieved with a localised galvanic anode was tested on a real-size specimen. One of the elements was taken from the building and was available for experimental tests in the laboratory. Results from these tests are presented in Redaelli et al. 2013. They showed that a single galvanic zinc anode positioned at one end of the specimen could produce a cathodic polarisation higher than 100 mV on steel reinforcement over a distance

of 0.3 m both in condition of water-saturation (where the current supplied by the anode was 500 μA) and in condition with 60% RH (where the current supplied by the anode was 80 μA). Hence, assuming the 100-mV decay criterion the height of protection of the anode was around 0.6 m, which means that protection of reinforcement on a real full-scale element could be achieved placing an anode every 0.6 m (i.e. 1.7 anodes every meter) along the height in the front part of the element. In the case analysed, this amount of anode per length of element could be considered acceptable.

These encouraging results were, then, further investigated by means of numerical models, that will be presented in this paper, with the aim of optimising the anodic configuration. First, small specimens were obtained from the real element and were used to characterise concrete and steel in relation to corrosion and to provide input parameters for numerical models. Then, calculations were carried out considering different scenarios by varying conditions and parameters that could not be controlled during experimental real-size tests, such as electrochemical conditions of steel, number and position of anodes, and concrete properties in terms of moisture content and carbonation. The results obtained will be discussed in relation with the performance of two anodic configurations, with anode spacing of either 0.9 m or 0.45 m, in providing protection to corroding slender elements.

2 Characterisation of corrosion parameters

Several small specimens containing sections of two longitudinal bars were obtained by cutting the newel and were used to characterise the behaviour of steel in alkaline and carbonated concrete, both in free corrosion conditions and under cathodic polarisation with impressed current. Test duration was of the order of few weeks to few months.

The specimens had a simple prismatic geometry (as it is shown in Figure 2) with a height of 55-70 mm. A MMO (*mixed metal oxide*) activated titanium mesh (of the type commonly used for impressed current *CP*) embedded in a layer of mortar was applied on a lateral surface of each specimen, parallel to rebars, in order to work as counter-electrode in electrochemical tests. The specimens were exposed to different conditions of humidity and were subjected to galvanostatic cathodic polarisation tests, with the aim of investigating the correlation between applied current and steel potential under cathodic polarisation. Free corrosion potential

and linear polarisation resistance of steel were measured on a reference specimen. The specimens and the sequence of tests are reported in Table 1. All potentials were measured versus an external SCE (*saturated calomel electrode*) reference electrode placed on the top surface of the specimen, as indicated in Figure 2. During the application of current, four-hour depolarisation tests were carried out in order to determine the *on* potential (E_{on}, measured during application of the current), the *instant-off* potential (E_{off}, measured within 1 s from switching off the current) and the *four-hour* potential (E_{4h}, measured after 4 hours from switching off the current). The difference between E_{4h} and E_{off} gives the four-hour potential decay.

Figure 3 shows, as an example, the results of potential measurements obtained on specimen A-1, which was subjected to a constant cathodic current of 5 mA/m^2 in various environments. In this specimen the steel was active since it was in contact with carbonated concrete. E_{on}, E_{off} and E_{4h} potentials are reported together with the applied cathodic current density. During the initial period of immersion, E_{on} and E_{off} potentials were -0.62 and -0.61 V/SCE, respectively; the small difference between them reflects a low ohmic drop contribution, due to the relatively low value of applied current and to the condition of immersion that makes concrete electrical resistivity low. E_{4h} potential was -0.58 V/SCE and the 4h decay was around 40 mV. When the specimen was exposed to a dry environment (50% RH), it progressively dried out. E_{on} decreased to values as low as -1.55 V/SCE, while E_{off} decreased to -0.64 V/SCE and its average value during exposure to dry environment was -0.55 V/SCE. E_{4h} was around -0.42 V/SCE and 4h decay was about 135 mV. Finally, after exposure to 95% RH, both E_{on} and E_{off} became more positive, and the 4h decay was around 80 mV.

The results obtained from all the specimens are summarised in Table 1 in terms of *instant-off* potential (E_{off}) and feeding voltage (ΔV); average values are reported, calculated from all values in each condition. E_{off} values were then plotted, together with literature data, versus the cathodic current density, as reported in Figure 4, with the aim of investigating the cathodic behaviour of steel in alkaline and carbonated concrete and, specifically, highlighting possible differences according to the conditions of carbonation of concrete. Although the scatter of the results, no systematic trend was observed in terms of potential versus current

density values in carbonated and alkaline concrete. Concrete carbonation did not play a primary role in the determination of the cathodic polarisation curve.
Also four plain concrete specimens without reinforcement (cubic geometry with side of approximately 45 mm) were cut from the newel and were used to determine the humidity content and the electrical resistivity in different conditions of humidity. After initial immersion, they were exposed in sequence to 90%, 50% and 95% relative humidity (RH) at temperature of 20°C. The electrical conductance, *C*, was measured between two parallel surfaces with a conductimeter; concrete resistivity, ρ, was obtained through the relation: $\rho = A/(C \cdot L)$, where *A* is the surface and *L* the thickness. During exposure to conditions of immersion, 95% and 90% RH, the moisture contents in concrete measured at the end of each exposure period were around 4%, 1.5% and 1%, respectively, and corresponding values of electrical resistivity were 40÷70 Ω·m, 350÷550 Ω·m and 110÷425 Ω·m. Values of concrete resistivity of 3900÷10000 Ω·m were measured during exposure to 50% RH. These results are representative of alkaline concrete, since it was not possible to obtain wholly carbonated specimens due to the relatively low depth of carbonation. Figure 5 shows the correlation between moisture content and resistivity measured on all the specimens. Values of resistivity higher than 1000 Ω·m, which is usually considered as a threshold value above which the propagation of carbonation induced corrosion can be neglected (Polder et al. 2000; Alonso et al. 1988), were obtained for moisture contents lower than 0.5%.

3 Current distribution

After characterising the corrosion conditions and the cathodic behaviour of steel in concrete on small samples, numerical simulations were performed with the aim of determining the distribution of current in a newel subjected to cathodic protection with localised galvanic anodes. The commercial package COMSOL was used. The soundness of numerical solutions as well as non-dependence on mesh size were checked for all models.

3.1 Description of element

The real newel is a precast concrete element reinforced with steel bars and wires. The shape is quite complex, thinner in the central part compared to the top and bottom ends (Figure 1). The front and rear parts are respectively 2.62 and 2.09 m high and 235 and 165 mm deep. The thickness varies between 60 and 120 mm; the lower thickness is in the centre of the front part. The front part is exposed outside; the rear part is embedded between adjacent elements such as panels and pillars and is not accessible.

Thanks to cutting of the newel in the top and bottom parts to obtain previously described specimens (§2), the position of the rebars and the carbonation depth were measured directly on several freshly-cut sections.

The reinforcement consists of two adjacent longitudinal bars (ϕ = 6 mm) in the front part of the element, and two (ϕ = 8 mm) in the rear part, anchored to each other with several twisted and bent steel wires (ϕ = 5 mm) placed at various heights (stirrups). In the top and bottom front parts, the longitudinal bars are bent up over a length of approximately 300 mm. All reinforcement is unribbed. Neither longitudinal bars nor wires are exactly parallel to the surface, giving rise to variability in concrete cover thickness.

Carbonation depths were measured with phenolphthalein tests and ranged between 17 and 30 mm on all sides; these values were somewhat lower compared to those expected after condition evaluation (Bertolini et al. 2009), indicating that in the newel most of reinforcement is still passive, being in contact with alkaline concrete, while many newels in the building are carbonated up to the depth of the bars. Only longitudinal rebars in the thinner part of the newel are in contact with carbonated concrete.

3.2 Geometry of the model

In spite of slight differences in the shape and variability of the position of reinforcement, the geometry determined on the newel was considered representative of most elements, and, therefore, it was used to define the geometry of the domain that was considered to simulate current distribution (Figure 6*a*).

The 3D domain reflected the geometry evaluated on the newel, with minor simplifications (e.g. the position of the longitudinal reinforcement and of the

anchoring wires). The concrete cover thickness on the front surface was set to 27 mm.

3.3 Scenarios

Various scenarios in terms of moisture content and carbonation of concrete and two different anodic configurations were considered.

Regarding humidity conditions, it was assumed that in the front part of the element, which is exposed to the atmosphere, concrete could be dry (moisture content in concrete around 0.5%), wet (around 1.5%) or saturated (around 4%), whilst in the rear part, which is in contact with adjacent elements, concrete was always considered dry. Regarding carbonation, it was assumed that the element could be fully carbonated, fully alkaline, or alkaline in the rear part and carbonated in the front part. The sharp division between front and rear, although not fully representative of real conditions, stemmed from the need to simplify the geometry of the subdomains.

The anodic configurations were defined in terms of number and position of anodes, consisting of small rods made of zinc and placed in the front part transversally to the lateral surface, at different heights, as indicated in Figures 6*b* and 6*c*. The rod has a width of 30 mm, a height of 5 mm and a length equal to the thickness of the newel. Experimental results on real-size specimen clearly showed that more than one anode is necessary to protect the element. Since in very aggressive (water-saturated) conditions the required anode spacing was 0.6 m (Redaelli et al. 2013), two anodic configurations were defined, with anode spacing of 0.9 m (i.e. three anodes per element) and of 0.45 m (i.e. six anodes per element). Configurations with anode spacing lower than 0.45 m, that require more than six anodes per element, were not considered realistic and, so, were not taken into account.

Selected combinations of the above-mentioned conditions of carbonation and moisture and anode configurations gave rise to the various scenarios considered, that are reported in Table 2. These scenarios were implemented by values of resistivity of concrete and boundary conditions of steel and anode surfaces, as it will be explained in the following section.

3.4 Input parameters

The numerical model requires the knowledge of the parameters that describe the electrochemical behaviour of steel and anode, and the electrical properties of the concrete, in the different scenarios. The parameters were selected both on the basis of the results obtained with experimental tests described in §2 and from literature values (Redaelli et al. 2006).

The electrochemical behaviour of steel was described through a Butler-Volmer type polarisation curve, in the form of:

$$i = i_{corr} \times 10^{\frac{(E-E_{corr})}{b_A}} - i_{corr} \times 10^{\frac{-(E-E_{corr})}{b_C}} \qquad \text{Eq. 1}$$

where i_{corr} is the free corrosion current density (in mA/m^2), E_{corr} the free corrosion potential (in V), and b_A and b_C the slopes of the anodic and cathodic branches of the curve (in V/dec). These four parameters were chosen as a function of the properties of concrete with which steel was in contact, in terms of carbonation and humidity content (expressed as resistivity).

A single cathodic curve was chosen for all cases, with a slope of 0.2 V/dec (without any limiting current of oxygen diffusion), in accordance with results obtained on small specimens (§2). For active steel, after selecting a given combination of free corrosion potential and corrosion rate (lying on the cathodic curve), the slope of the anodic branch of the curve was determined by intersection with the point with potential of -1 V/SCE and current density of 0.01 mA/m^2, i.e. roughly the equilibrium potential and exchange current density of the reaction of iron oxidation, as it is shown in Figure 7. This is consistent with the anodic resistive control that characterises the corrosion of steel in carbonated concrete (Glass et al. 1991). Specifically, for active steel in carbonated and wet concrete a free corrosion potential of -0.36 V/SCE and a free corrosion current density of 2 mA/m^2 were selected, that resulted in an anodic slope of 0.28 V/dec, while for active steel in carbonated and dry concrete a potential of -0.1 V/SCE and current density of 0.1 mA/m^2 were selected, and the resulting anodic slope was 1 V/dec. In carbonated and water-saturated concrete the corrosion current density was 5 mA/m^2 and the resulting cathodic slope was 0.21 V/SCE. For passive steel, the anodic slope was set to 1000 V/dec, giving a vertical anodic branch that was intended to represent the condition of passivity. All the parameters are summarised in Table 3.

For the boundary conditions on the galvanic anode, a constant potential value was assumed, equal to -1.05 V/SCE, which is a typical potential value for zinc in contact with an alkaline environment (de Rincón et al. 1997).[1]
Finally, the electrical resistivity of concrete was specified as a function of concrete carbonation and moisture content. According to literature data the resistivity of carbonated concrete was assumed to be 4-10 times greater than that of alkaline concrete in the same condition of exposure (Anstice et al. 2005; Dias 2000; Mo 2012; Ngala and Page 1997; Polder 2001). So, the resistivity of alkaline concrete was set to 250 Ω·m in wet condition and 400 Ω·m in dry condition; the resistivity of carbonated concrete was set to 1000 Ω·m in wet condition, 10000 Ω·m in dry condition and 200 Ω·m in water-saturated condition (Table 3).

3.5 Results

Figures 8 and 9 show examples of the distributions of potential (*a*) and current density (*b*) along the height of reinforcement in the front part and in the rear part of a newel protected with three and six anodes ("bent front" indicates the bent part of longitudinal bars in the front part, as depicted in Figure 6*a*; the potential of stirrups is not shown). These results refer to the scenario in which the newel is fully carbonated and it is wet in the front part and dry in the rear part.
The longitudinal rebars in the front part of the newel show an uneven potential distribution: in the presence of three anodes they are cathodically polarised only in the vicinity of the anodes, where their potential is about -0.5 V/SCE, while between the anodes their potential is close to -0.36 V/SCE, i.e. the free corrosion value (dashed black line); bent reinforcement shows somewhat lower values of potential due to its closeness to the anode. Also in the case with six anodes the potential is -0.5 V/SCE in the vicinity of the anodes, while it is -0.4 V/SCE far from the anodes. The longitudinal rebars in the rear part, that are farther from the anodes compared to those in the front, show a more uniform potential distribution, with values around -0.25 V/SCE close to the anodes and -0.2 V/SCE in between anodes in the configuration with three anodes and almost constant with values of -0.33÷-0.3 V/SCE in the configuration with six anodes (for these rebars the free

[1] Galvanic anodes made of zinc are encased in a highly alkaline electrolyte in order to keep the metal active. The potential chosen for zinc anodes reflects the contact with such alkaline environment.

corrosion potential is -0.1 V/SCE as indicated by the dashed grey line). These rebars do not require to be protected from corrosion, since they are in contact with dry concrete, anyway they have to be considered since they receive a current due to the electrical connection with the bars in the front part of the element.

The current density on the front bars approaches values of 10 mA/m^2 in the vicinity of the anodes in both configurations, while far from the anodes it is of the order of 0.1 mA/m^2 or even less when three anodes are used and 1 mA/m^2 when six anodes are used; the reinforcement in the rear part receives a much more even current density in the range 0.2÷0.4 mA/m^2 in both cases.

The results of all simulations are summarised in Tables 4 and 5. As a general trend, the most negative potential and the maximum current density are always obtained on reinforcement portions close to the anodes. Moreover, potential and current density distributions on the rear reinforcement are more uniform compared to those on the front reinforcement. Decreasing anode spacing from 0.90 m to 0.45 m considerably affects the most positive value of steel potential on the front reinforcement (which decreases), while the effect on the most negative value is negligible.

Table 6 shows the current supplied by each anode and the total anodic current; in each scenario differences in the current supplied by each single anode are mainly due to geometric differences inside the element, related to anode dimension and position. In the cases where calculations for both anodic configurations are available, the current supplied by each anode is slightly lower in the configuration with anode spacing of 0.45 m, and so the total current supplied by six anodes is slightly less than twice the total current supplied by three anodes. In general, for a given anodic configuration, when the concrete in the front part is dry, the current supplied by the anodes is lower compared to wet or water-saturated concrete.

With anode spacing of 0.45 m, the highest current is supplied when the concrete in the front part is water-saturated, and it is of the order of 3000-3150 μA. A high anodic current (2750 μA) is also supplied when the element is fully alkaline, and wet in the front part, whilst if it is fully dry the current is much lower (250 μA). When the element is completely carbonated, the total current is around 800 μA when the concrete in the front is wet and 110 μA when the concrete in the front is dry.

5 Discussion of results

The performance of a galvanic *CP* system with localised anodes needs to be investigated in relation with two main aspects: the distribution of potential, that determines the protection to steel reinforcement, and the consumption of anodes, that determines their working life. The numerical simulations allow to determine current and potential distributions in the presence of galvanic anodes and, therefore, to evaluate the effectiveness of the two anodic configurations in protecting steel reinforcement from corrosion in slender elements. In the following, protection conditions will be addressed with regard to the reinforcement in the front part of the element; the reinforcement in the rear part is characterised by a low corrosion risk, since it is either passive (being in contact with alkaline concrete), or active (being in contact with carbonated concrete) in conditions of lack of humidity that prevent corrosion propagation. The presence of the rear reinforcement, however, cannot be completely neglected since it affects the current the anodes supply, and, as a consequence, their performance in time.

5.1 Protection of reinforcement

In §4 results of numerical simulations were presented in terms of distribution of potential and current density on the reinforcement. However, the effectiveness of the protection provided by a cathodic current is not directly correlated with these parameters: measurements carried out on the reinforcement of a real element showed that, for a given applied cathodic current, steel potential strongly depends on concrete moisture content, and it is much more nagative in wet concrete compared to dry concrete, although not indicating a higher protection level (Redaelli et al. 2013). So, the results were analysed in terms of cathodic polarisation, i.e. the difference between the free corrosion potential and the potential in the presence of the anodes, and in terms of anodic activity of steel, i.e. the current density evaluated on the anodic polarisation curve at the potential value reached by the steel (Figure 10). The cathodic polarisation has a practical relevance, since it is related to the cathodic depolarisation usually measured in cathodic protection systems (as previously proposed by Polder et al. 2009); the anodic activity is a measure of the corrosion rate of steel under polarisation, and can be useful to estimate the expected delay of cracking of concrete and, hence, increase of service life after the intervention.

As an example, Figure 11 shows the distribution of cathodic polarisation on the front reinforcement in the case of fully carbonated element, wet in the front part; the bar chart on the right indicates areas with cathodic polarisation higher than 100 mV (white), lower than 50 mV (black) and intermediate (grey). Close to each anode (indicated by a circle) there is a portion of reinforcement where the cathodic polarisation is higher than 100 mV; each of these portions is surrounded by an area where the cathodic polarisation is between 50 and 100 mV and, finally, in positions far from the anodes, the polarisation is lower than 50 mV. Although protection conditions on real structures are usually evaluated only through cathodic polarisation, simulations also allow an estimation of the actual anodic activity of steel along the protected bar. The corrosion rate was evaluated in a similar way and it was classified as lower than 1 mA/m^2 (negligible value), between 1 and 2 mA/m^2 (intermediate) and higher than 2 mA/m^2 (high corrosion rate). The results obtained from these classifications are shown in Figures 12 and 13 that depict intervals of cathodic polarisation and corrosion rate of steel, respectively, in all the scenarios.

The configuration with anode spacing of 0.90 m cannot be considered adequate to protect corroding elements. As a matter of fact, in the scenarios where concrete is carbonated and wet, the height with a cathodic polarisation higher than 100 mV around each anode is 0.05÷0.1 m, which means an overall height of 10% with respect to the total length of the reinforcement. The percentage where the cathodic polarisation is higher than 50 mV is 25%. Considering the corrosion rate, values lower than 1 mA/m^2 characterise 15% of reinforcement, while values lower than 2 mA/m^2 characterise 80-90% of reinforcement. So, both criteria of cathodic polarisation and corrosion rate indicate an incomplete protection of actively corroding steel reinforcement.

When anode spacing is reduced to 0.45 m, the amount of reinforcement with cathodic polarisation higher than 100 mV increases in each scenario, not only because the number of anodes is higher, but also because their reduced spacing is such that reinforcement at intermediate position between two anodes receives current from both. For instance, considering the case when the element is carbonated and wet in the front and alkaline and dry in the rear, the height with cathodic polarisation higher than 100 mV around a single anode is 0.1÷0.2 m. This can be attributed to a more even distribution of current (that can also be seen,

for instance, comparing Figures 8 and 9), and not to a higher amount of current supplied by each anode. In fact, as already mentioned, the current supplied by each anode is slightly lower when there are six anodes instead of three (Table 6).

Neglecting scenarios in which concrete is fully dry (either alkaline or carbonated), where cathodic polarisation is always higher than 50 mV and corrosion rate is always lower than 1 mA/m^2, it can be observed that if the carbonated element is wet in the front there are regions with cathodic polarisation lower than 50 mV, which are however characterised by corrosion rate lower than 2 mA/m^2. However, when concrete in the front is temporarily water-saturated, the corrosion rate reaches values well higher than 2 mA/m^2 in spite of a relatively favourable distribution of cathodic polarisation that is mainly higher than 50 mV.

Comparing the conditions of water-saturated concrete and wet concrete, two contrasting factors clearly emerge: on one hand, the promotion of current circulation in saturated concrete due to low electrical resistivity, and, on the other hand, the hindrance of protection conditions due to the high corrosion rate of steel in saturated concrete. The former results in a higher percentage of steel polarised more than 100 mV in the more severe condition of water-saturation; the latter results in a higher rate of propagation of corrosion, due to the higher corrosion rate of steel.

The condition of concrete in the rear part affects the distribution of potential in the front part as a consequence of variation in electrical resistivity: for instance, in the scenarios where concrete in the front part is carbonated and saturated, the cathodic polarisation is always higher than 50 mV if concrete in the rear part is alkaline (resistivity of 400 Ω·m), while it shows areas lower than 50 mV if concrete in the rear part is carbonated (resistivity of 10000 Ω·m). Conversely, the condition of steel bars in the rear part (active or passive) only affects the current circulating between them and the anode.

The protection conditions depicted in Figures 12 and 13 are conservative since the evaluation of both cathodic polarisation and corrosion rate according to Figure 10 neglects possible long-term effects of cathodic protection such as the repassivation of steel due to the alkalinity produced by the applied current, which is expected to be beneficial even for relatively low applied current (Bertolini et al. 2003; Redaelli and Bertolini 2011). On the short term, such changes have been observed as well (Pacheco et al. 2011).

Moreover, in accordance with the polarisation curves reported in Figure 7, values of cathodic polarisation equal to or higher than 100 mV guarantee that the corrosion rate of steel is below 2 mA/m^2 even in very aggressive (water-saturated and carbonated) conditions. In less aggressive environments, such as in carbonated and wet concrete, even a cathodic polarisation of 50 mV is representative of protection of steel. To this regard it should be noted that the standard on cathodic protection of steel in concrete does not explicitly require a depolarisation higher than 100 mV for galvanic anode systems (EN ISO 12696 2012).

Figure 12 also shows that should a condition of cathodic polarisation higher than 100 mV be required on the entire front reinforcement in all the exposure conditions considered, the anode spacing should be lower than 0.45 m. However, this requirement could be relaxed considering that:

- the height of protection obtained from numerical simulations is more conservative compared to that measured on a real-size element, owing to several factors as the presence of an alkaline core with lower resistivity that enhances current distribution (this was verified through numerical simulations carried out on the same real-size element, not presented here),
- the most severe conditions (water-saturation in the front part of a completely carbonated element) are unlikely to occur on real elements,
- even wet conditions are reached only for limited (rainy) periods,
- the long-term beneficial effects of the cathodic current, such as the production of alkalinity, are neglected in the numerical simulations (that only consider “static” short-term scenarios).

If so, given the necessity to limit the number of anodes, the configuration with six anodes can be considered suitable to protect the steel reinforcement from carbonation-induced corrosion, provided possible differences in exposure conditions and extent of carbonation are properly taken into account.

5.2 Consumption of anodes

In addition to the protection of reinforcement from corrosion, an effective *CP* system should be able to work properly for the intended service life, typically 10-20 years, during which the anodic system has to supply sufficient current (Polder and Peelen 2011). Therefore, also the behaviour in time of the anodic system has

to be taken into account, in particular for galvanic anodes whose working life may be limited by their consumption (Sergi 2011; de Rincón et al. 2008). Table 6 reports the theoretical consumption rate of each anode *r* (obtained by Faraday's law supposing that the anodic current is constant in time and assuming 100% anode efficiency) and its theoretical working life *t* (obtained as the ratio between the mass of each anode and its consumption rate).

Referring to the configuration with anode spacing of 0.45 m, the lowest durations are around 16-18 years and are obtained in carbonated and water-saturated concrete. Such durations could be increased, to some extent, increasing the anode mass: given the small anode size, its volume can be increased leaving current distribution practically unchanged. When concrete is carbonated and wet the durations are 60-95 years. When the element is completely dry, either alkaline or carbonated, very long durations of at least 200 years are obtained. However, even if the alkaline element is wet in the front, the consumption rates are such that the durations are 18-27 years, i.e., for the same conditions, much lower than for fully carbonated element. This indicates that galvanic anodes are self-regulating, but not so smart to supply current only when needed, since they consume even when the steel does not need to be protected. This suggests that a convenient repair strategy should be based on the preliminary determination of elements that really need protection, rather than on the systematic application of anodes to all elements.

Reinforcement in the rear part, which is always in contact with dry concrete, also contributes to anode consumption. Table 7 reports the cathodic current received by the reinforcement, distinguishing between reinforcement in the front part (continuous and bent longitudinal), reinforcement in the rear part and stirrups (which are roughly half in the front and half in the rear, see Figure 6). The fraction of current on the rear reinforcement is 15-20%. This contribution to anode consumption cannot be eliminated due to the electrical contact amongst reinforcement.

Previous estimates are "static" since they refer to a hypothetical condition that does not change in time. In real conditions of exposure, the elements are subject to wetting-drying cycles and, as a consequence, their moisture content changes in time. Also micro-climatic conditions (e.g., local shelter from rain) affect the actual moisture content in the element and its evolution in time. Based on data from the

weathering station close to the building considered in this work, it can be assumed that each year there are 160 rainy days, 10 of which are consecutive with intensity higher than 2.5 mm. As a consequence, the front part can be assumed to be dry for 205 days, wet for 150 days and saturated for 10 days each year. The duration of the anodes in real exposure conditions can be estimated with these average annual values. For instance, referring to the case when the element is fully carbonated and is protected with six anodes, results shown in Table 8 are obtained. Values equal to or higher than 100 years are obtained even for the end-anodes. It should be reminded that these values only refer to the consumption of the anodic material; in real conditions, further factors (not considered here) may affect the duration of the anodic system, such as the effectiveness of the encasing material that keeps the anode active, or the electrical connection to the steel.

6 Conclusions

A combined experimental and numerical study was carried out to investigate the possibility of protecting slender reinforced concrete elements from carbonation-induced corrosion using few small localised galvanic anodes.

Galvanostatic cathodic polarisation tests on steel in concrete in various conditions of carbonation and humidity allowed to determine the cathodic polarisation curve that was used as an input in numerical simulations.

The current distribution obtained allowed to evaluate the effectiveness of two anodic configurations (anode spacings of 0.90 m and 0.45 m) in protecting steel reinforcement and to make predictions on the long-term behaviour of the anodes in relation with their consumption.

The configuration with anode spacing of 0.90 m (three anodes in the case considered) is not suitable due to incomplete protection of portions of reinforcement that are far from the anodes.

The configuration with anode spacing of 0.45 m (six anodes) is suitable for the protection of the reinforcement from corrosion: although a cathodic polarisation higher than 100 mV can not be obtained in all the corroding scenarios considered, when the concrete is wet the corrosion rate is kept lower than 2 mA/m^2; when it is water-saturated, portions of steel with corrosion rate higher than 2 mA/m^2 are present, however these conditions are unlikely to occur for more than few days each year.

Estimated anode durations are of the order of several tens or even hundreds of years, except when concrete is water-saturated or when it is alkaline and wet, where durations are lower than 20 years. Also reinforcement in contact with dry concrete, even in the rear part of the element, that does not need to be protected from corrosion, contributes to anode consumption. Hence, in order to avoid extra costs of repair and waste of materials, it seems appropriate to use a galvanic anode *CP* system only where and when corrosion has initiated and propagates due to carbonation.

Acknowledgements. This study was financed by CIS-E, Milan.

References

Alonso C, Andrade C, Gonzales JA (1988) Relation between resistivity and corrosion rate of reinforcements in carbonated mortar made with several cement types. Cement Concrete Res 18(5):687-698

Anstice DJ, Page CL, Page MM (2005) The pore solution phase of carbonated cement pastes. Cement Concrete Res 35(2):377-383. doi: 10.1016/j.cemconres.2004.06.041

Bennett JE, Turk T, Tettamanti M, Manghi M, Tremolada S (2008) Testing STARGARD™ discrete anodes for concrete. In: Proc. Eurocorr 2008, 7-11 September, Edinburgh UK

Bertolini L, Bolzoni F, Pastore T, Pedeferri P (1998) Cathodic protection of reinforcement in carbonated concrete. In: Proc. Corrosion/98, paper 639, NACE, Houston, pp 1-13

Bertolini L, Pedeferri P, Redaelli E, Pastore T (2003) Repassivation of steel in carbonated concrete induced by cathodic protection. Mater Corros 54(3):163-175. doi: 10.1002/maco.200390036

Bertolini L, Lollini F, Redaelli E (2009) Corrosion assessment of structural and decorative reinforced concrete of Torre Velasca in Milan. In: Mazzolani FM (ed) Proc. Int. Conf. PROHITECH 09, 21-24 June, Rome, Taylor and Francis Group, London, pp 495-500

Dias WPS (2000) Reduction of concrete sorptivity with age through carbonation. Cement Concrete Res 30(8):1255-1261

EN ISO 12696 Standard (2012) Cathodic protection of steel in concrete

Glass GK, Page CL, Short NR (1991) Factors affecting the corrosion rate of steel in carbonated mortars. Corros Sci 32(12):1283-1294

Heinemann HA, van Hees RPJ, Nijland TG (2008) Concrete: Too young for conservation? In: Fodde E (ed) Structural analysis of historic construction: preserving safety and significance. Proc. of the VI Int. Conf. SAHC08, 2-4 July, Bath UK, CRC Press, pp 151-159

Holmes SP, Wilcox GD, Robins PJ, Glass GK, Roberts AC (2011) Responsive behaviour of galvanic anodes in concrete and the basis for its utilisation. Corros Sci 53(10):3450-3454. doi: 10.1016/j.corsci.2011.06.026

Jordan LC, Page CL (2003) Mortars for encapsulating sacrificial zinc anodes in reinforced concrete. Mater Corros 54(6):387-393. doi: 10.1002/maco.200390088

Lambert P (1995) Cathodic protection of reinforced concrete. Anti-Corros Methods Mater 42(4):4-5

Macdonald S (2003) The investigation and repair of historic concrete. NSW Heritage Office

Matthews S (2007) CONREPNET: Performance-based approach to the remediation of reinforced concrete structures: Achieving durable repaired concrete structures. J Build Apprais 3(1):6-20. doi: 10.1057/palgrave.jba.2950063

Mo L, Panesar DK (2012) Effects of accelerated carbonation on the microstructure of Portland cement pastes containing reactive MgO. Cement Concrete Res 42(6):769-777. doi: 10.1016/j.cemconres.2012.02.017

Ngala VT, Page CL (1997) Effects of carbonation on pore structure and diffusional properties of hydrated cement pastes. Cement Concrete Res 27(7):995-1007

Pacheco J, Polder RB, Fraaij ALA, Mol JMC (2011) Short-term benefits of cathodic protection of steel in concrete. In: Grantham M, Mechtcherine V, Schneck U (eds) Proc. Concrete Solutions, Dresden, Taylor and Francis, pp 147- 156

Pedeferri P (1996) Cathodic protection and cathodic prevention. Constr Build Mater 10(5):391-402

Polder RB (1998) Cathodic protection of reinforced concrete structures in The Netherlands - experience and developments, Cathodic protection of concrete - 10 years experience. Heron 43(1):3-14

Polder RB (2001) Test methods for on site measurement of resistivity of concrete - a RILEM TC-154 technical recommendation. Constr Build Mater 15(2-3):125-131. doi: 10.1016/S0950-0618(00)00061-1

Polder RB, Peelen WHA, Lollini F, Redaelli E, Bertolini L (2009) Numerical design for cathodic protection systems for concrete. Mater Corros 60(2):130-136. doi: 10.1002/maco.200805056

Polder R, Andrade C, Elsener B,Vennesland Ø, Gulikers J, Weidert R, Raupach M (2000) Test methods for on site measurement of resistivity of concrete. Mater Struct 33(10):603-611

Polder RB, Peelen WHA (2011) Service life aspects of cathodic protection of concrete structures. In: Grantham M (ed) Concrete repair, A practical guide, Taylor and Francis, Abingdon, pp 248-261

Redaelli E, Bertolini L (2011) Electrochemical repair techniques in carbonated concrete. Part II: cathodic protection. J Appl Electrochem 41(7):829-837. doi: 10.1007/s10800-011-0302-3

Redaelli E, Bertolini L, Peelen W, Polder R (2006) FEM-models for the propagation of chloride induced reinforcement corrosion. Mater Corros 57(8):628-635. doi: 10.1002/maco.200603994

Redaelli E, Carsana M, Gastaldi M, Lollini F, Bertolini L (2011) Electrochemical techniques for the repair of reinforced concrete suffering carbonation-induced corrosion. Corros Rev 29(5-6):179-190. doi: 10.1515/CORRREV.2011.008

Redaelli E, Lollini F, Bertolini L (2013) Throwing power of localised anodes for the cathodic protection of slender carbonated concrete elements in atmospheric conditions. Constr Build Mater 39:95-104. doi: 10.1016/j.conbuildmat.2012.05.014

de Rincón OT, Hernández-López Y, de Valle-Moreno A, Torres-Acosta AA, Barrios F, Montero P, Oidor-Salinas P, Montero JR (2008) Environmental influence on point anodes performance in reinforced concrete. Constr Build Mater 22(4):494-503. doi: 10.1016/j.conbuildmat.2006.11.014

de Rincón OT, de Romero MF, de Carruyo AR, Sánchez M, Bravo J (1997) Performance of sacrificial anodes to protect the splash zone of concrete piles. Mater Struct 30(9):556-560

Schiessl P, ed (1994) RILEM Technical Committee 124-SRC, Draft recommendation for repair strategies for concrete structures damaged by reinforcement corrosion. Mater Struct 27(7):415-436

Sergi G (2011) Ten-year results of galvanic sacrificial anode in steel reinforced concrete. Mater Corros 62(2):98-104. doi: 10.1002/maco.201005707

Sitton I, Powers RG, Costa JE (1998) Galvanic metalized zinc cathodic protection system for a carbonated reinforced concrete structure. In: Proc. Corrosion/98, paper 645, NACE, Houston, pp 1-14

Tables

Table 1 Summary of results from tests on small samples in different exposure conditions: applied cathodic current density, average instant off potential (E_{off}) and average feeding voltage (ΔV)

Specimen (steel condition)	Exposure period (day)	Exposure condition	Current density (mA/m^2)	E_{off} (V/SCE)	ΔV (min/max) (V)
P-1 (passive)	30	50% RH	10*	-0.427	14.8 (3.01/26.7)
	10	Immersion	10	-0.456	1.039
	40	Immersion	5	-0.463	0.791
	20	Immersion	-	-0.377	-
P-2 (passive)	30	Immersion	10	-0.534	1.142
	10	Immersion	5	-0.470	1.025
	20	Immersion	100	-0.711	2.610
	20	Immersion	10	-0.446	1.124
	20	Immersion	-	-0.330	-
A-1 (active)	28	Immersion	5	-0.613	1.127
	10	50% RH	5	-0.553	1.894
	27	95% RH	5	-0.575	1.566
A-2 (active)	28	Immersion	10	-0.743	1.321
	10	50% RH	10	-0.776	3.749
	27	95% RH	10	-0.715	2.345
A-3 (active)	14	Immersion	10	-0.628	1.165
	14	Immersion	100	-1.080	2.39
	10	50% RH	100*	-2.240	25.27 (18.74/26.82)
	27	95% RH	100	-0.959	5.3
A-4 (active)	14	Immersion	100	-1.160	2.457
	14	Immersion	10	-1.026	1.620
	10	50% RH	10	-0.770	3.885
	27	95% RH	10	-0.729	1.80
A-5 (active)	40	Immersion	-	-0.616**	-

* nominal value that could not be supplied due to saturation of generator

** average free corrosion rate = 5.46 mA/m^2

Table 2 Scenarios considered in the numerical simulations (sat. = saturated)

Reinforcement	*Concrete in the rear part*	*Concrete in the front part*	*Anode spacing*	
			0.90 m	*0.45 m*
Completely passive steel	Alkaline, dry	Alkaline, dry		×
	Alkaline, dry	Alkaline, wet		×
Active steel in the front part and passive steel in the rear part	Alkaline, dry	Carbonated, wet	×	×
	Alkaline, dry	Carbonated, sat.		×
Completely active steel	Carbonated, dry	Carbonated, dry	×	×
	Carbonated, dry	Carbonated, wet	×	×
	Carbonated, dry	Carbonated, sat.		×

Table 3 Input parameters used in numerical simulations in different conditions of carbonation and humidity: for steel, parameters used in Eq.1; for concrete, electrical resistivity ρ

			Steel				Concrete
			E_{corr}	i_{corr}	b_A	b_C	ρ
Concrete	Condition	Label	(V/SCE)	(mA/m^2)	(V/dec)	(V/dec)	(Ω·m)
Carbonated	Wet	*C-W*	-0.36	2	0.28	0.2	1000
Carbonated	Saturated	*C-S*	-0.45	5	0.21	0.2	200
Carbonated	Dry	*C-D*	-0.1	0.1	1	0.2	10000
Alkaline	Wet	*A-W*	-0.15	0.2	1000	0.2	250
Alkaline	Dry	*A-D*	-0.15	0.2	1000	0.2	400

Table 4 Minimum and maximum values of steel potential on front, bent front, rear reinforcement and stirrups in the various scenarios

	Front	*A-D*	*A-W*	*C-W*	*C-S*	*C-D*	*C-W*	*C-S*
	Rear	*A-D*	*A-W*	*A-D*	*A-D*	*C-D*	*C-D*	*C-D*
Spacing	*Reinf.*	E_{min}/E_{max} *(mV/SCE)*						
0.90 m	front	-	-	-521/ -357	-	-347/ -117	-522/ -359	-
	bent front	-	-	-599/ -364	-	-430/ -127	-600/ -365	-
	rear	-	-	-320/ -245	-	-204/ -119	-273/ -203	-
	stirrups	-	-	-461/ -259	-	-275/ -121	-463/ -220	-
0.45 m	front	-412/ -249	-612/ -461	-554/ -416	-655/ -513	-350/ -183	-527/ -394	-695/ -466
	bent front	-489/ -265	-684/ -484	-630/ -435	-717/ -531	-429/ -198	-618/ -411	-736/ -498
	rear	-249/ -224	-330/ -304	-427/ -398	-338/ -313	-185/ -160	-333/ -287	-338/ -294
	stirrups	-375/ -236	-577/ -324	-520/ -412	-	-313/ -170	-494/ -302	-642/ -311

Table 5 Minimum and maximum values of cathodic current density on front, bent front, rear reinforcement and stirrups in the various scenarios

	Front	*A-D*	*A-W*	*C-W*	*C-S*	*C-D*	*C-W*	*C-S*
	Rear	*A-D*	*A-D*	*A-D*	*A-D*	*C-D*	*C-D*	*C-D*
Spacing	*Reinf.*	i_{min}/i_{max} *(mA/m^2)*						
0.90 m	front	-	-	0/ 9.1	-	0/ 1.2	0/ 9.2	-
	bent front	-	-	0.1/ 29.0	-	0/ 4.3	0.1/ 29.1	-
	rear	-	-	0.3/ 0.9	-	0/ 0.2	0/ 0.5	-
	stirrups	-	-	0/ 4.3	-	0/ 0.5	0/ 4.5	-
0.45 m	front	0.2/ 2.9	3.3/ 30.5	0.7/ 8.9	3.6/ 33.3	0.1/ 1.3	0.7/ 9.5	4.0/ 26.1
	bent front	0.3/ 13.8	5.1/ 123.7	1.2/ 37.6	5.6/ 137.0	0.1/ 6.2	1.2/ 35.9	9.2/ 134.2
	rear	0.2/ 0.3	0.6/ 5.0	0.2/ 0.4	0.7/ 1.3	0.07/ 0.14	0.2/ 0.3	0.3/ 0.6
	stirrups	0.2/ 1.8	0.6/ 20.2	0.3/ 6.0	-	0.1/ 0.8	0.2/ 6.5	0.2/ 17.2

Table 6 Current supplied by each anode and total anodic current (*I*, in μA), theoretical consumption rate (*r*, in g/year) and duration of the anode (*t*, in year), obtained from numerical simulations in the various scenarios. *H* is the position of the anodes (height in m in the front part). Labels are defined in Table 3

	Front	*A-D*	*A-W*	*C-W*	*C-S*	*C-D*	*C-W*	*C-S*
	Rear	*A-D*	*A-D*	*A-D*	*A-D*	*C-D*	*C-D*	*C-D*
Spacing	*H (m)*	*I (μA)*						
0.90 (m)	0.43	-	-	148	-	20	145	-
	1.31	-	-	100	-	13	98	-
	2.29	-	-	206	-	28	205	-
	total	-	-	454	-	61	448	-
0.45 (m)	0.22	64	681	193	776	28	204	745
	0.66	31	336	94	385	13	97	372
	1.10	31	345	97	395	14	100	377
	1.54	31	342	96	391	14	99	371
	1.98	41	447	126	510	18	131	477
	2.42	57	604	172	686	25	182	658
	total	255	2756	779	3143	112	814	3000
	H (m)	*r (g/year)*						
0.90 (m)	0.43	-	-	1.58	-	0.21	1.55	-
	1.31	-	-	1.07	-	0.14	1.05	-
	2.29	-	-	2.2	-	0.3	2.19	-
0.45 (m)	0.22	0.68	7.27	2.06	8.28	0.3	2.18	7.96
	0.66	0.33	3.59	1.01	4.11	0.14	1.04	3.97
	1.10	0.34	3.69	1.03	4.22	0.15	1.07	4.03
	1.54	0.33	3.65	1.03	4.18	0.14	1.06	3.96
	1.98	0.44	4.78	1.35	5.44	0.19	1.4	5.09
	2.42	0.61	6.45	1.83	7.33	0.27	1.94	7.03
	H (m)	*t (year)*						
0.90 (m)	0.43	-	-	81	-	603	83	-
	1.31	-	-	83	-	621	84	-
	2.29	-	-	58	-	428	59	-
0.45 (m)	0.22	189	18	62	16	428	59	16
	0.66	271	25	88	22	622	85	22
	1.10	264	24	86	21	606	83	22
	1.54	266	24	86	21	611	83	22
	1.98	291	27	95	24	668	92	25
	2.42	212	20	70	18	479	66	18

Table 7 Cathodic current (*I*, in μA) received by reinforcement in the front part of the element, in the rear part and on the stirrups

	Front	*A-D*	*A-W*	*C-W*	*C-S*	*C-D*	*C-W*	*C-S*
Spacing	*Rear*	*A-D*	*A-D*	*A-D*	*A-D*	*C-D*	*C-D*	*C-D*
0.90 (m)	Front	-	-	156	-	21	162	-
	Bent front	-	-	118	-	16	120	-
	Rear	-	-	46	-	7	27	-
	Stirrups	-	-	65	-	8	71	-
0.45 (m)	Front	85	1031	280	1166	37	297	1165
	Bent front	76	762	222	860	34	223	837
	Rear	28	98	36	110	12	29	48
	Stirrups	43	552	157	-	19	165	588

Table 8 Duration of the anode (*t*, in year) in fully carbonated concrete in variable conditions of exposure (concrete in the front is dry for 205 days, wet for 150 days and saturated for 10 days each year)

H (m)	*t (year)*
0.22	100
0.66	144
1.10	140
1.54	141
1.98	156
2.42	113

Captions for figures

Figure 1 Geometry of the newel (dimensions in mm)

Figure 2 Schematic geometry of specimens used in galvanostatic cathodic protection tests

Figure 3 Example of results of galvanostatic tests on specimen A-1. *On* (E_{on}), *instant-off* (E_{off}) and *four-hour* (E_{4h}) potentials of steel reinforcement and cathodic current density (*cd*) are shown

Figure 4 Instant off values of steel potential as a function of the applied cathodic current density, measured on steel in alkaline and carbonated concrete in different exposure conditions (circles refer to data from Bertolini et al. 2003)

Figure 5 Electrical resistivity of alkaline concrete as a function of moisture content measured on four plain specimens exposed to different conditions of relative humidity

Figure 6 3D geometry of element with reinforcement considered in numerical simulations (*a*), configuration with three anodes (*b*, bars not shown) and configuration with six anodes (*c*, bars not shown)

Figure 7 Determination of anodic slopes of steel in carbonated concrete in dry, wet and water-saturated conditions according to the cathodic curve (grey line) and to the free corrosion conditions (circles). Slopes are in V/dec

Figure 8 Distribution of potential (*a*) and current density (*b*) on steel reinforcement connected with three galvanic anodes placed at heights of 0.43, 1.31 and 2.29 m. Front part: carbonated and wet concrete; rear part: carbonated and dry concrete

Figure 9 Distribution of potential (*a*) and current density (*b*) on steel reinforcement connected with six galvanic anodes placed at heights of 0.22, 0.66, 1.1, 1.54, 1.98 and 2.42 m. Front part: carbonated and wet concrete; rear part: carbonated and dry concrete

Figure 10 Determination of cathodic polarisation and anodic activity of steel

Figure 11 Example of determination of ranges of cathodic polarisation on the reinforcement in the front part of a completely carbonated element (wet in the front, dry in the rear). The bar on the right shows heights where the cathodic polarisation is lower than 50 mV (black), between 50 and 100 mV (grey) and higher than 100 mV (white). Circles indicate anodes

Figure 12 Intervals of cathodic polarisation of steel bars in the front part of the newel in the various scenarios considered. Circles indicate the height of anode position (placed in the front part of the element)

Figure 13 Intervals of corrosion rate of steel bars in the front part of the newel in the various scenarios considered. Circles indicate the height of anode position (placed in the front part of the element)

Figure-01

Click here to download high resolution image

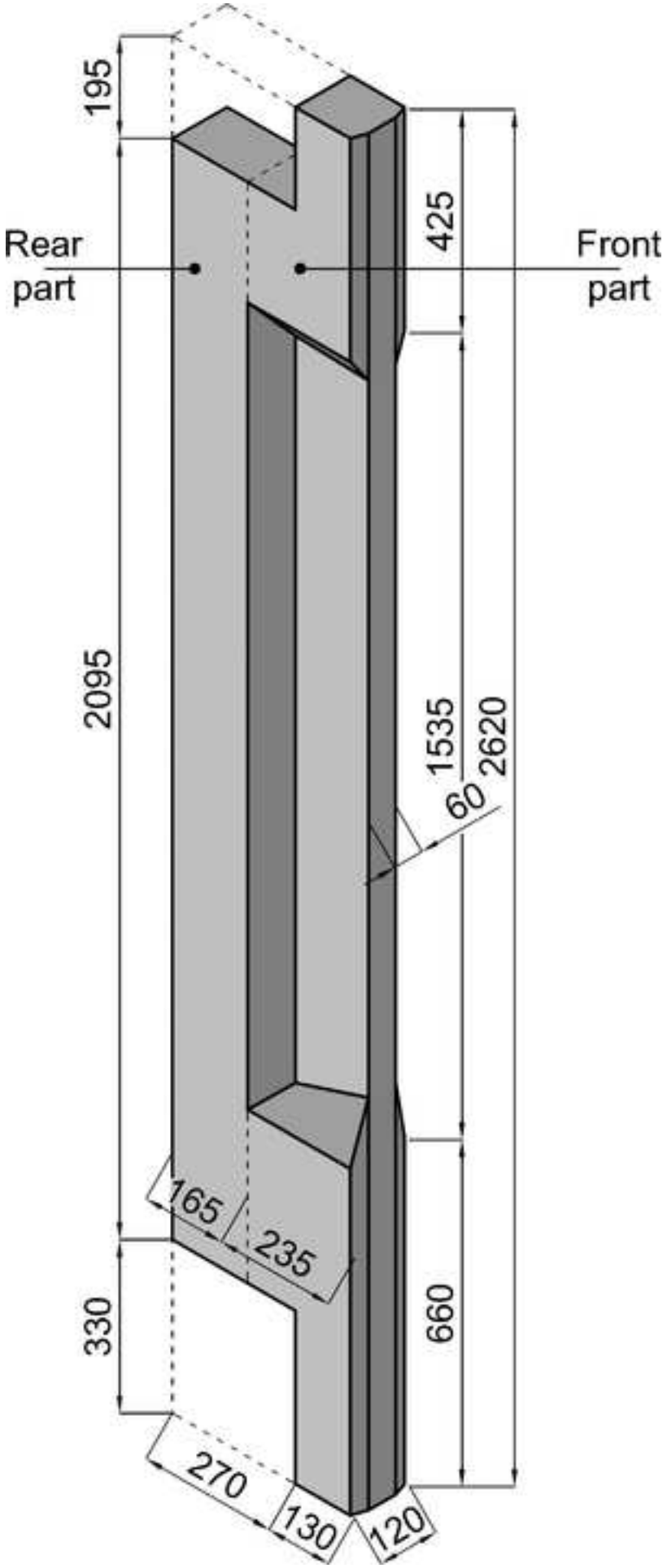

Figure-02
Click here to download high resolution image

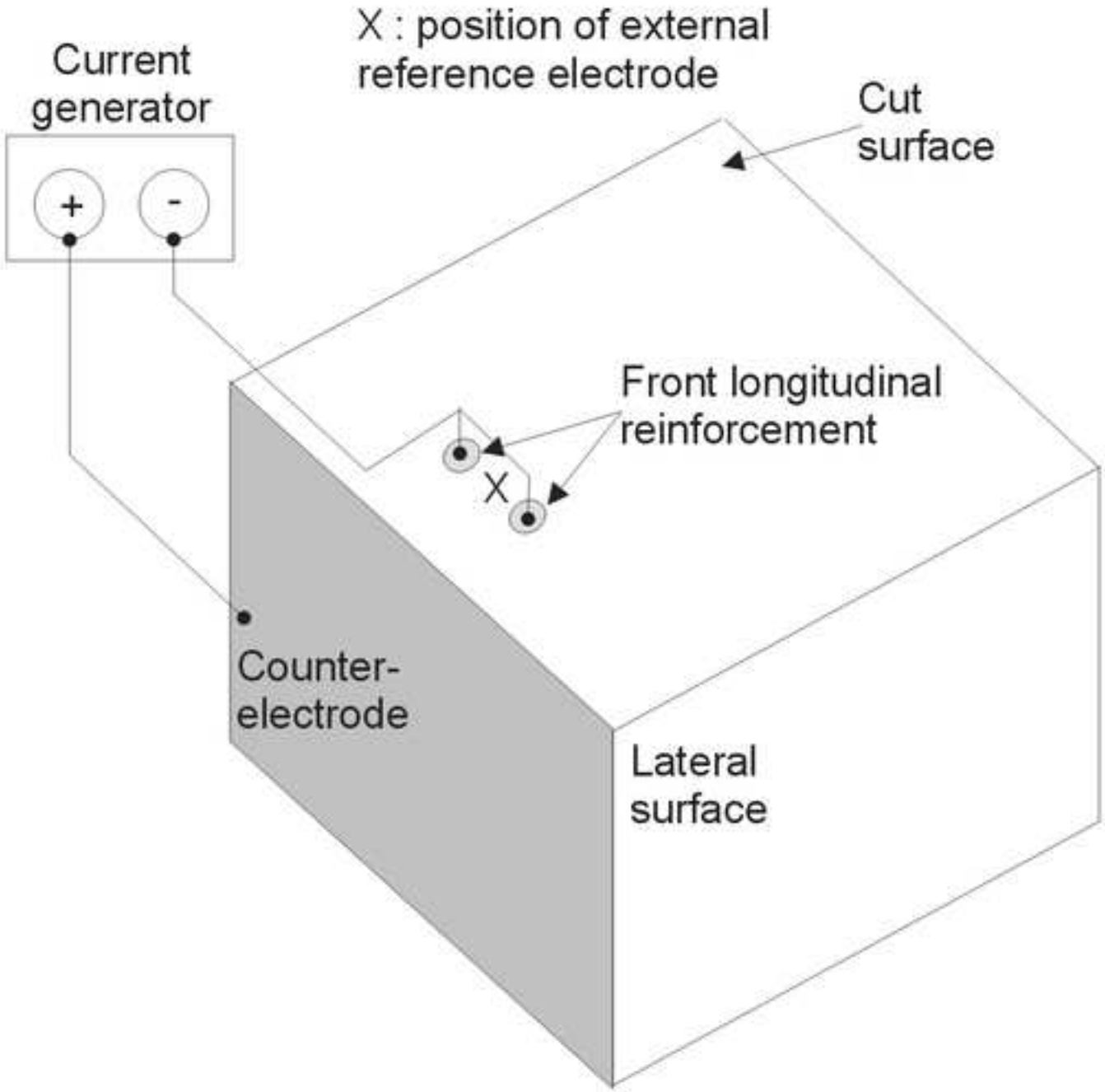

Figure-03
Click here to download high resolution image

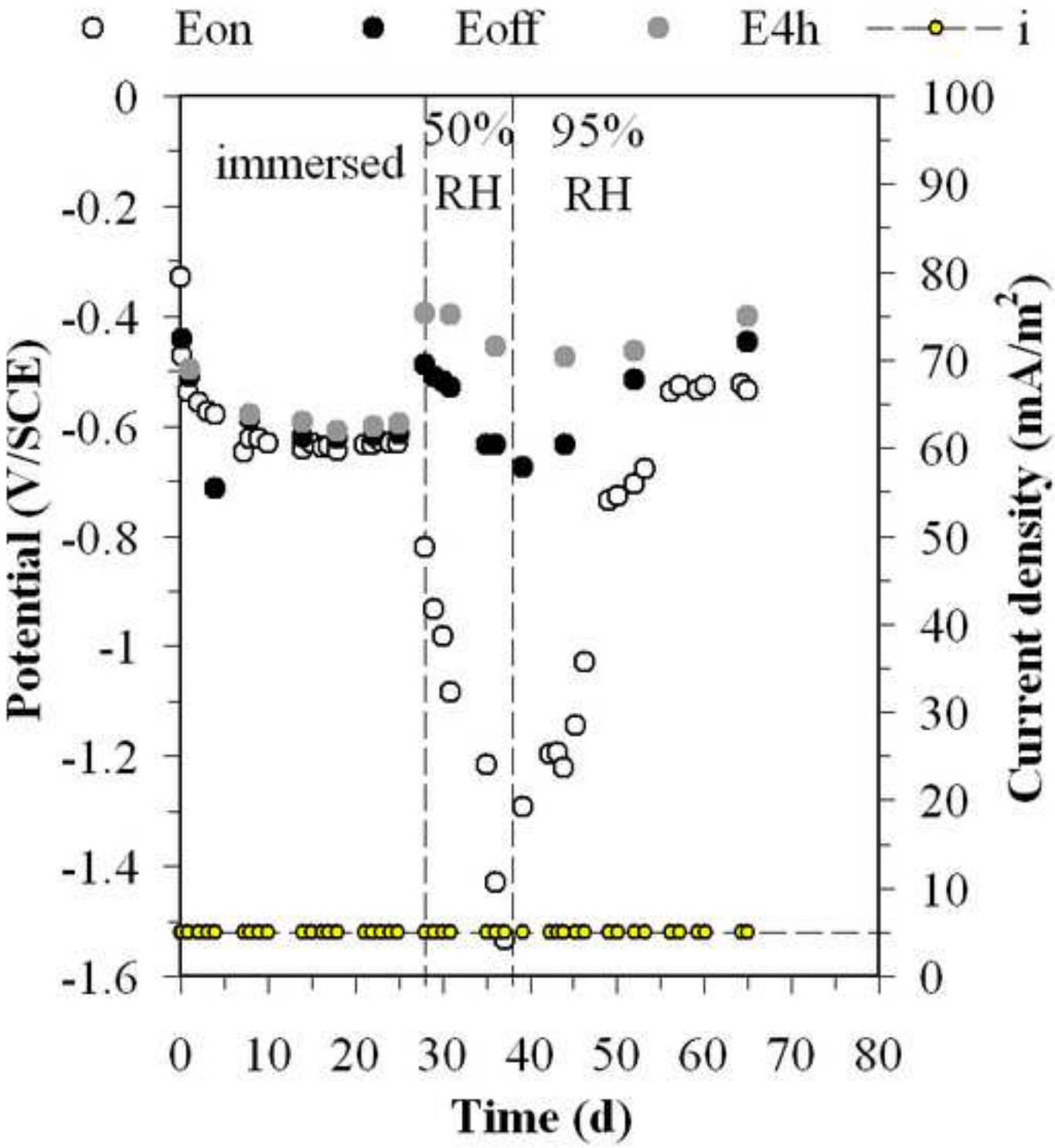

Figure-04

Click here to download high resolution image

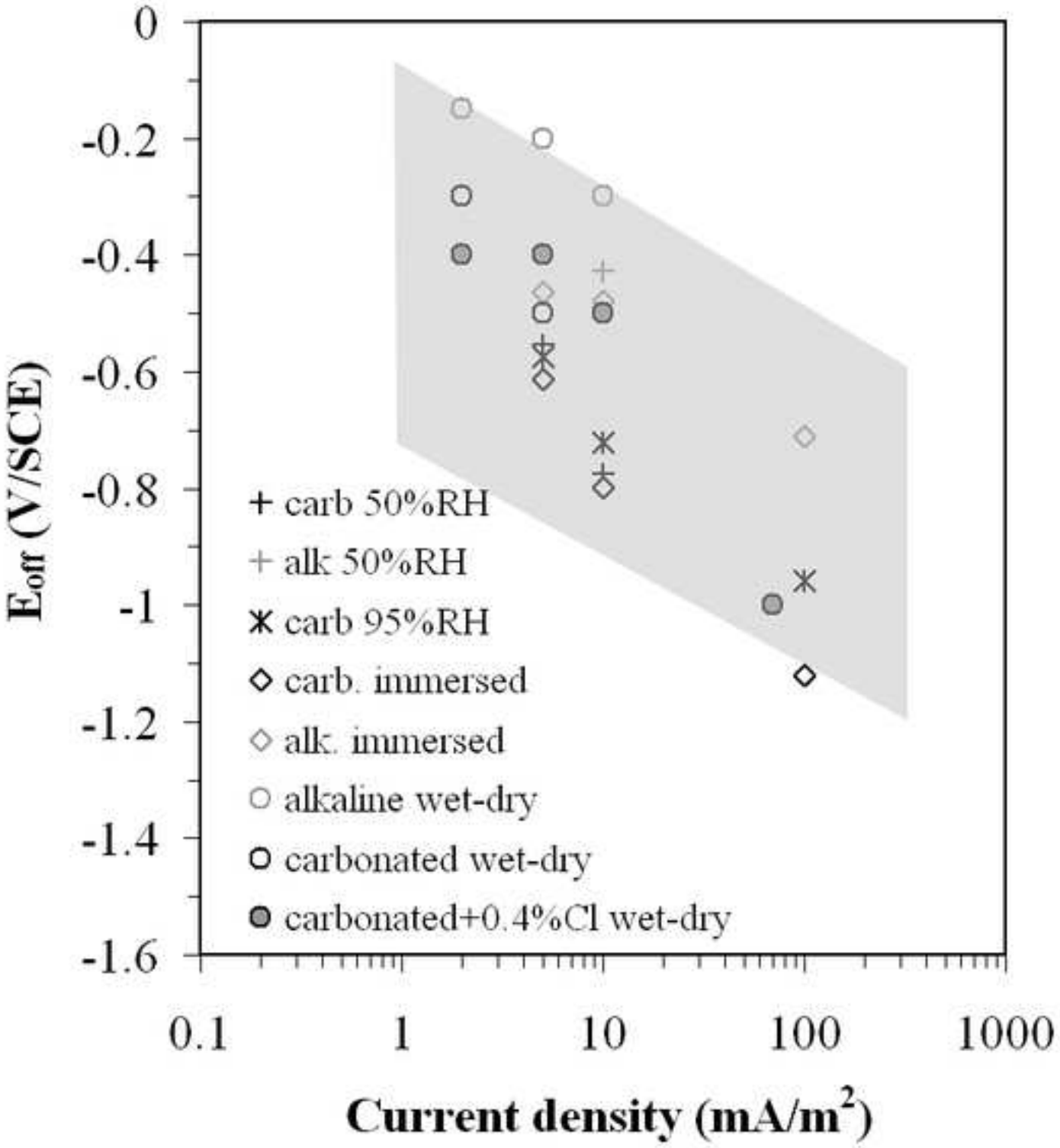

Figure-05

Click here to download high resolution image

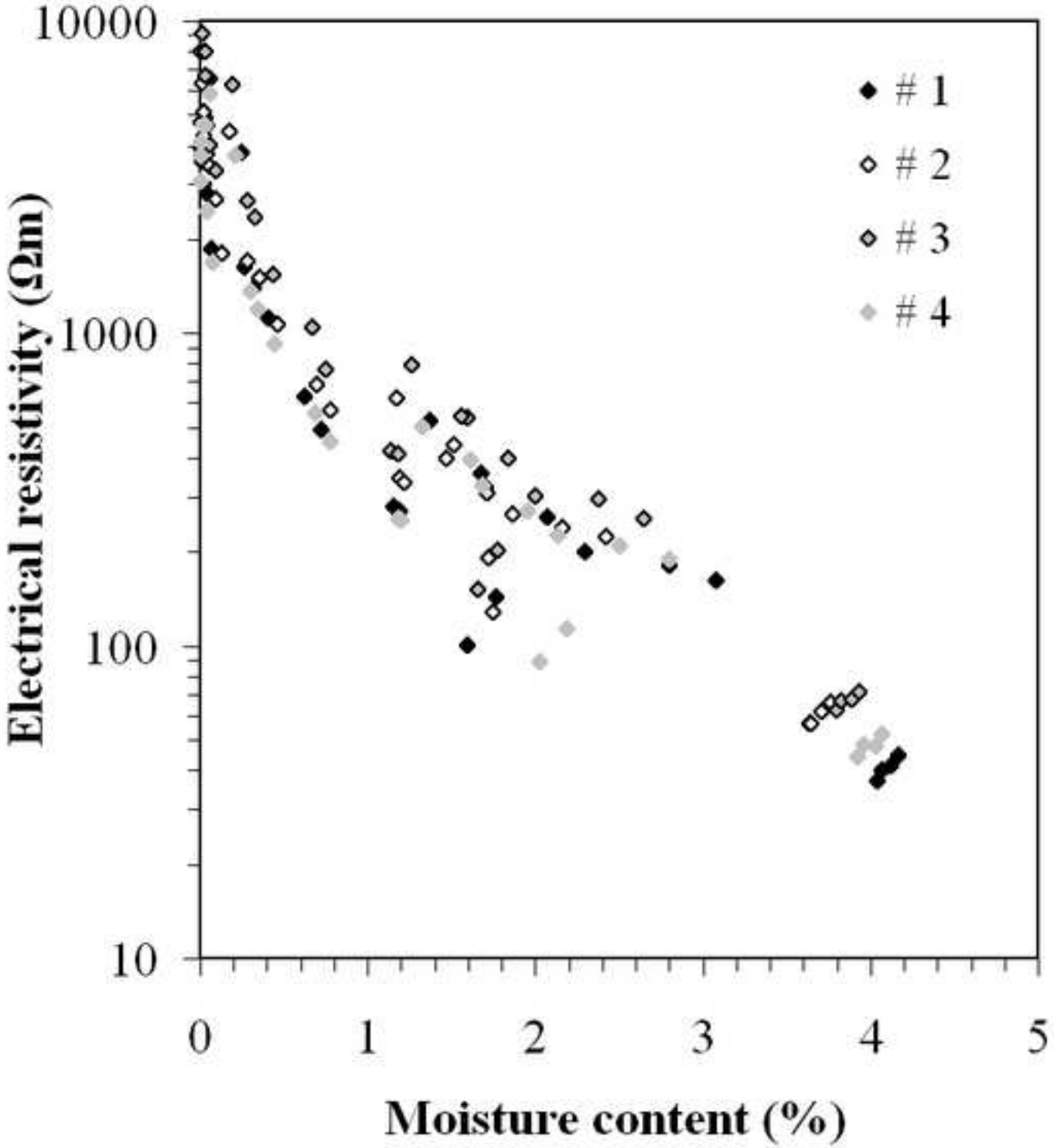

Figure-06

Click here to download high resolution image

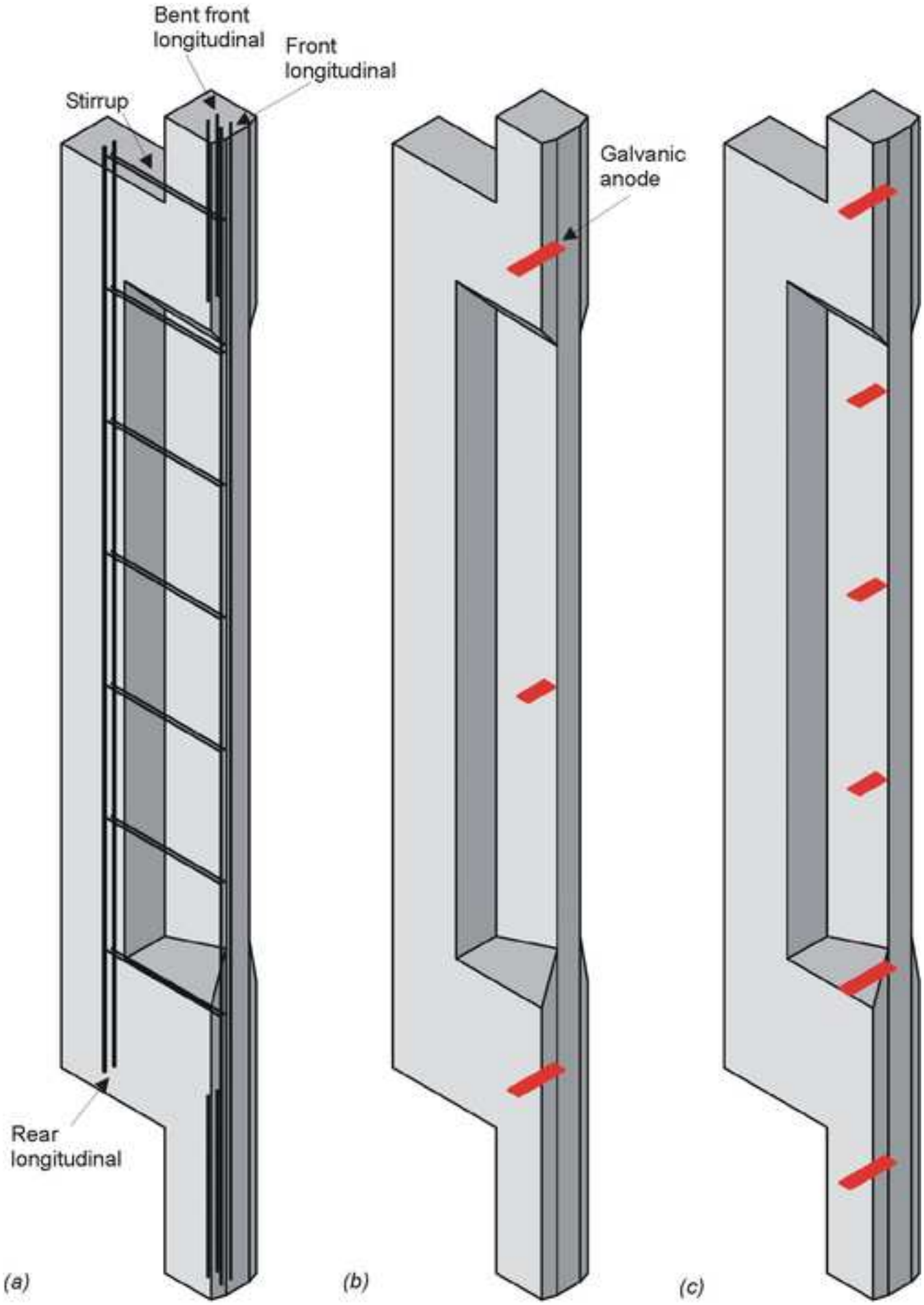

Figure-07

Click here to download high resolution image

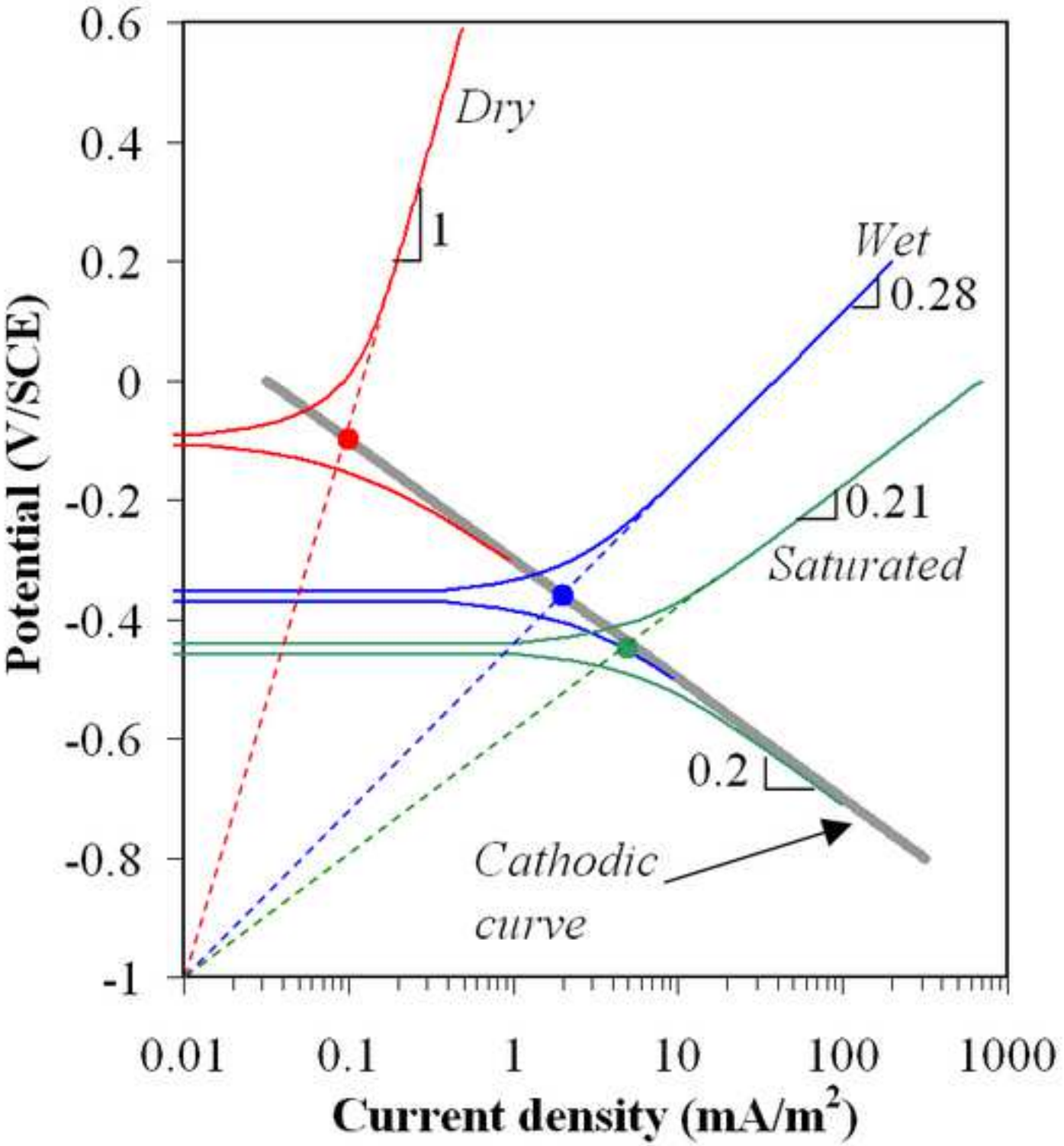

Figure-08-a

Click here to download high resolution image

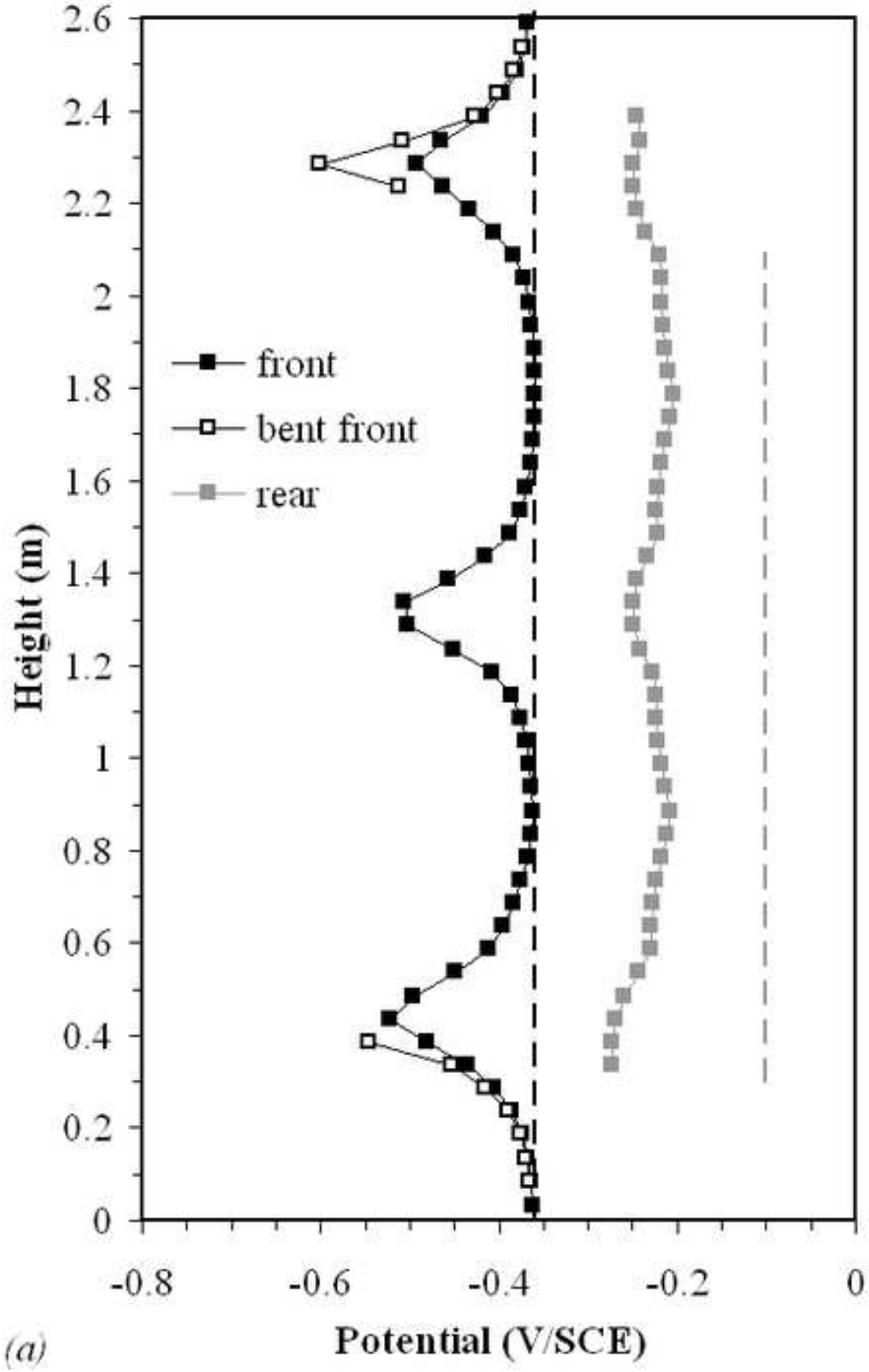

Figure-08-b

Click here to download high resolution image

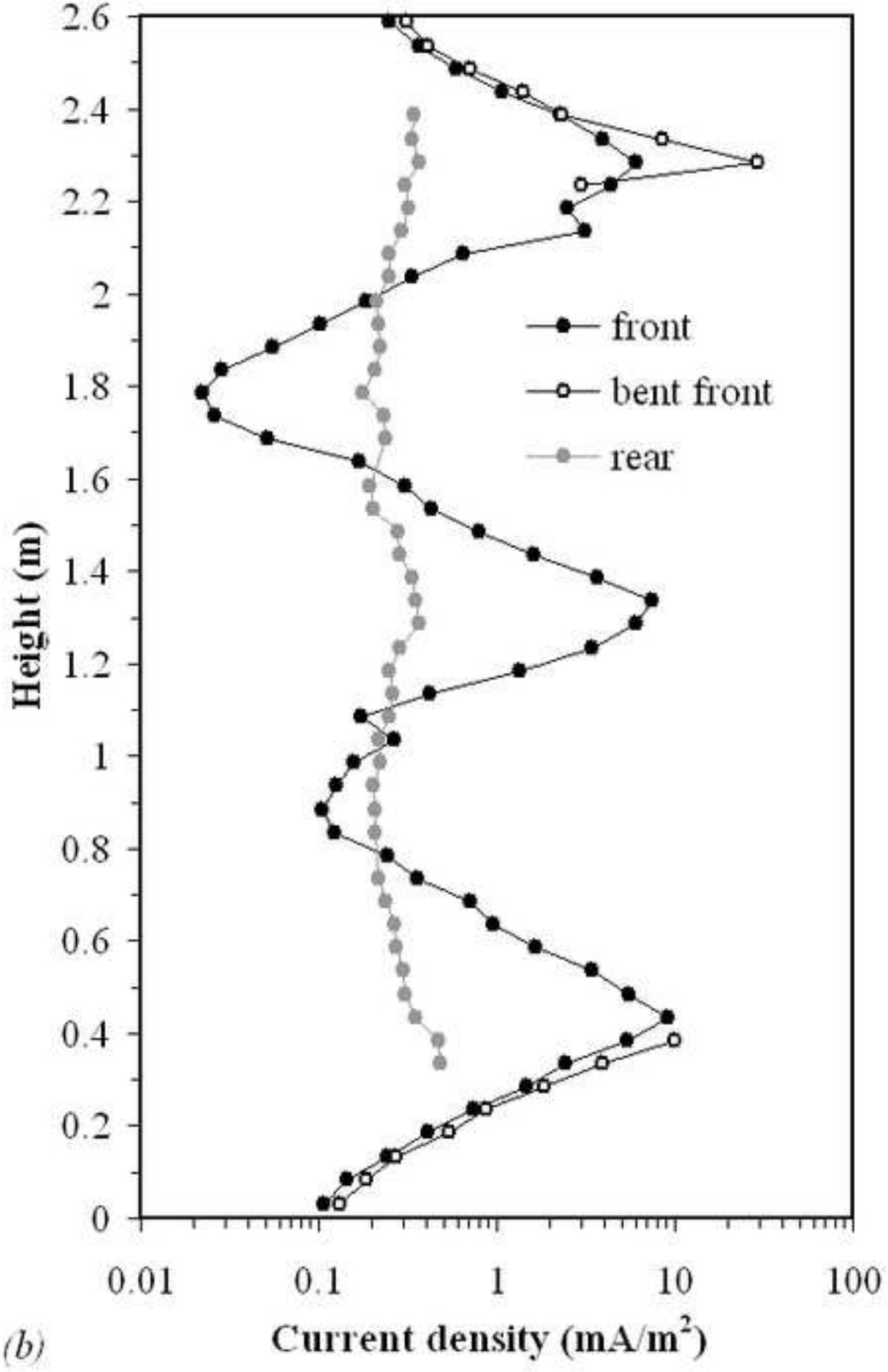

Figure-09-a

Click here to download high resolution image

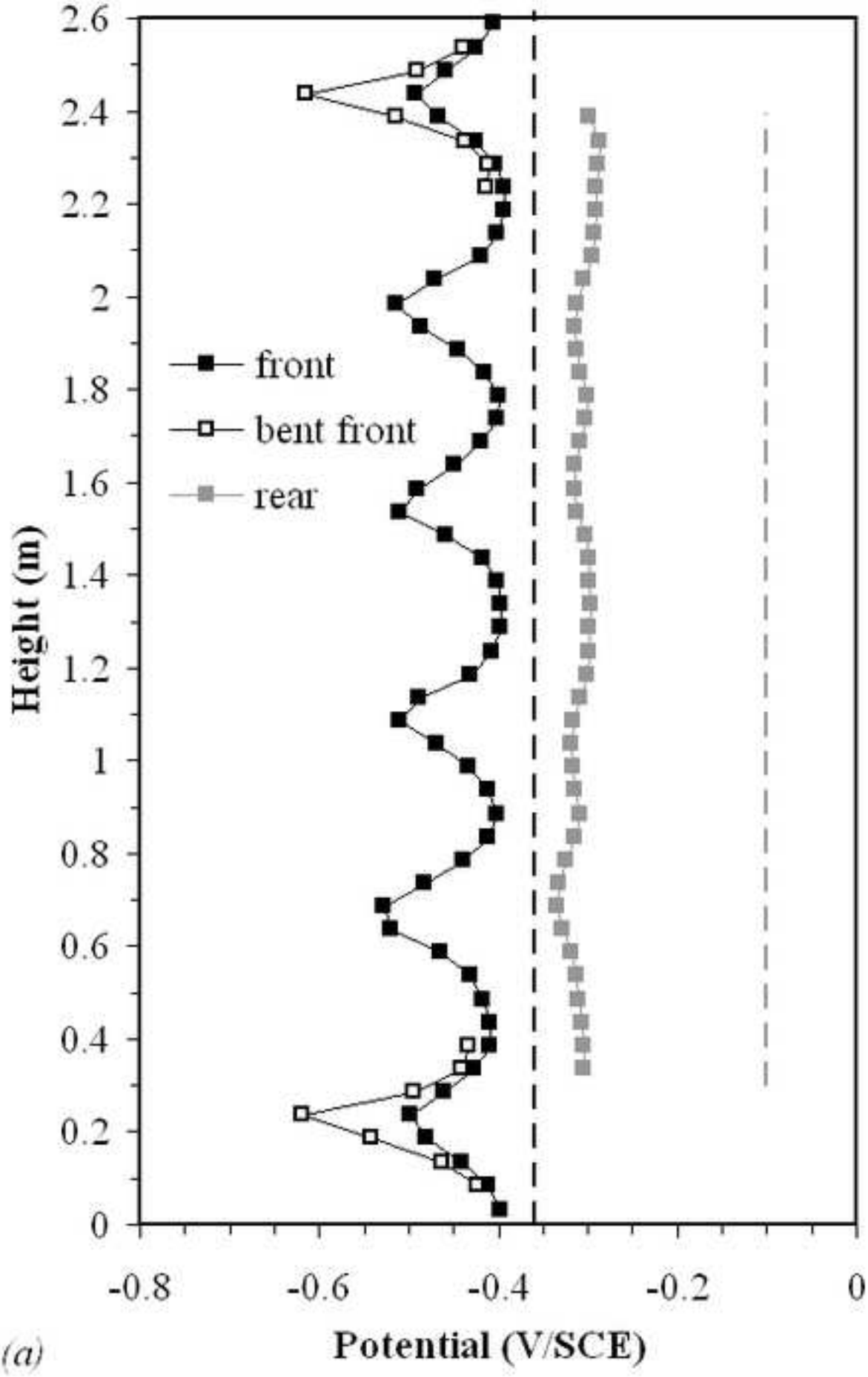

Figure-09-b

Click here to download high resolution image

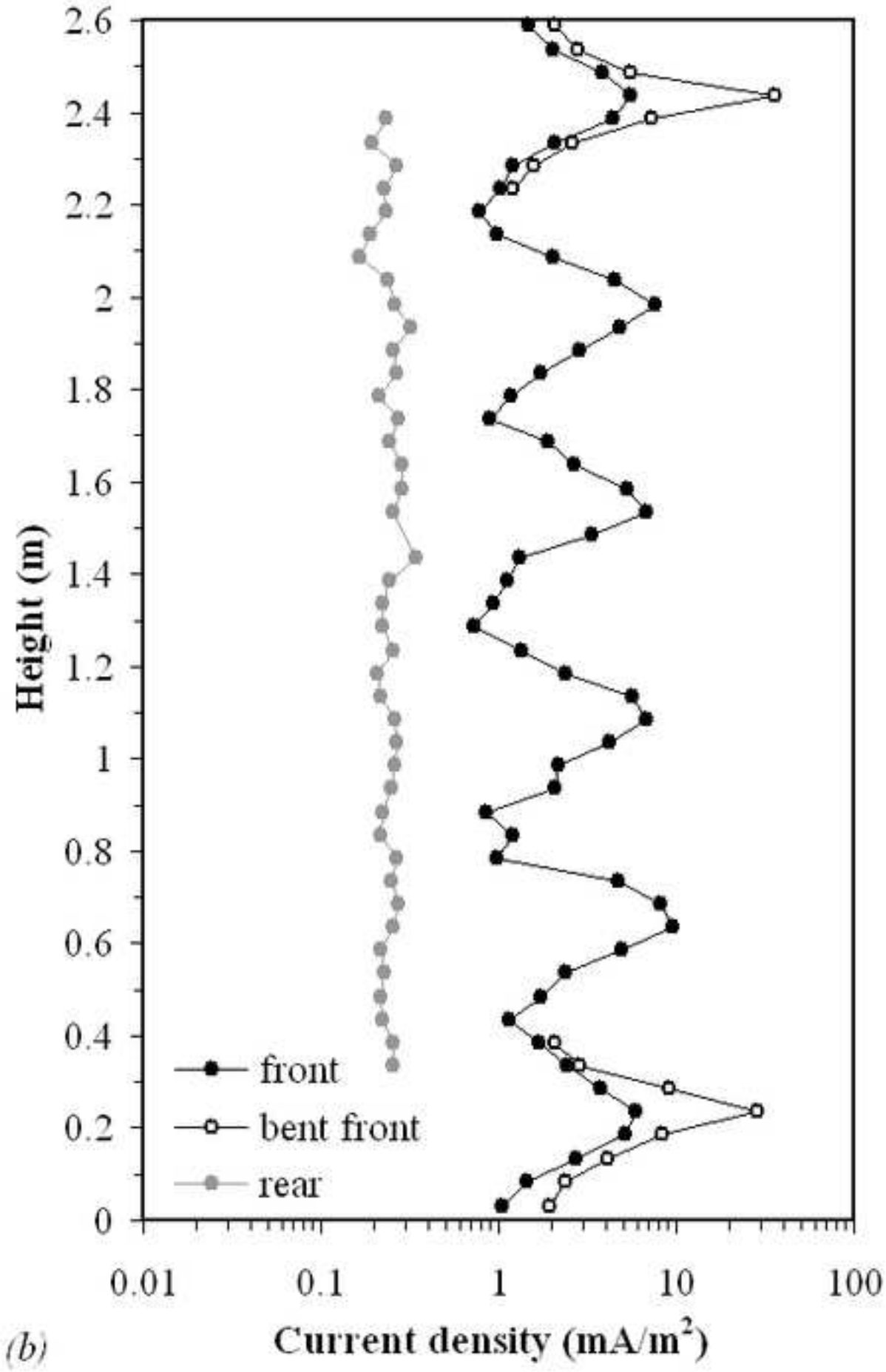

(b)

Figure-10
Click here to download high resolution image

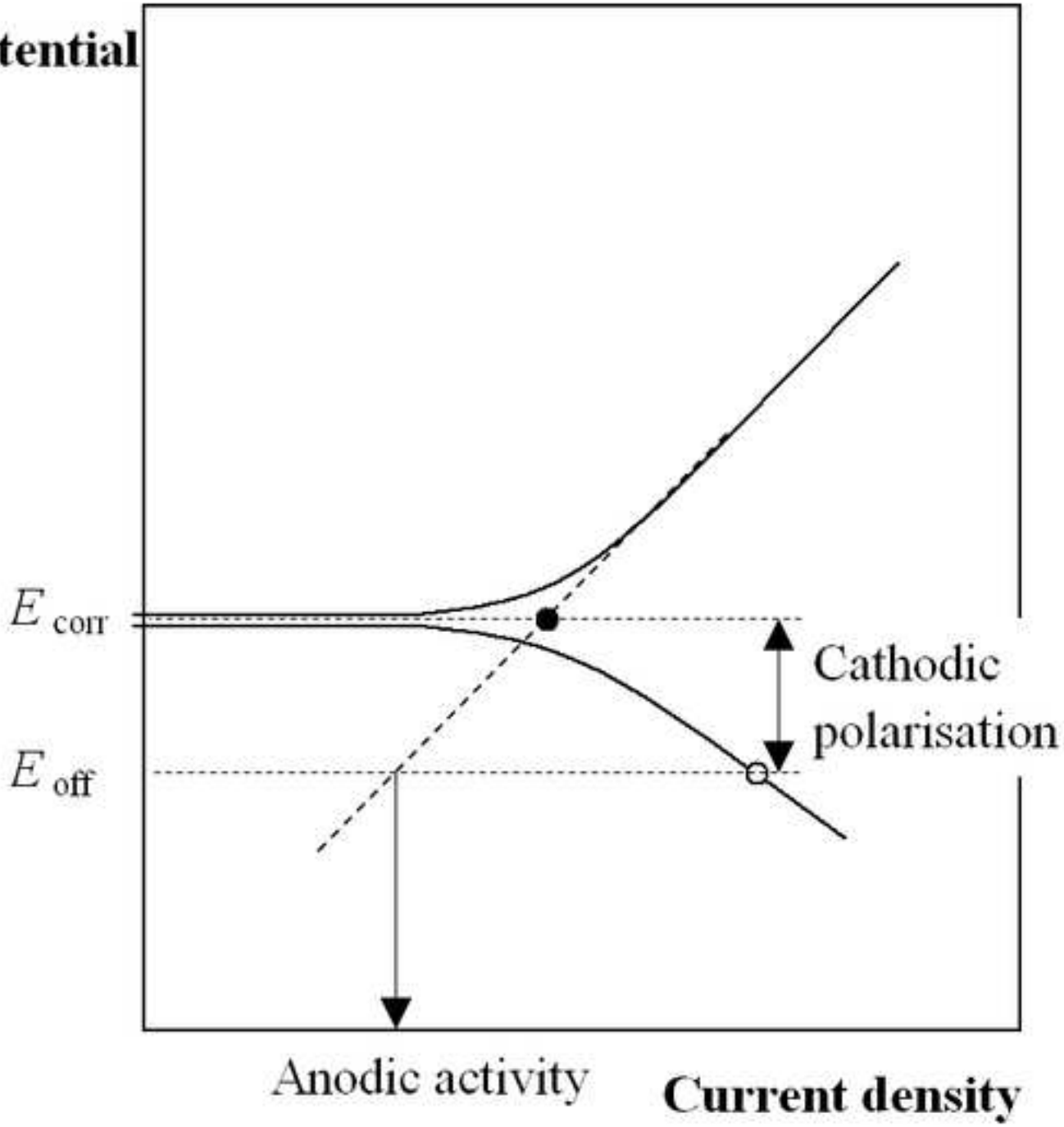

Figure-11
Click here to download high resolution image

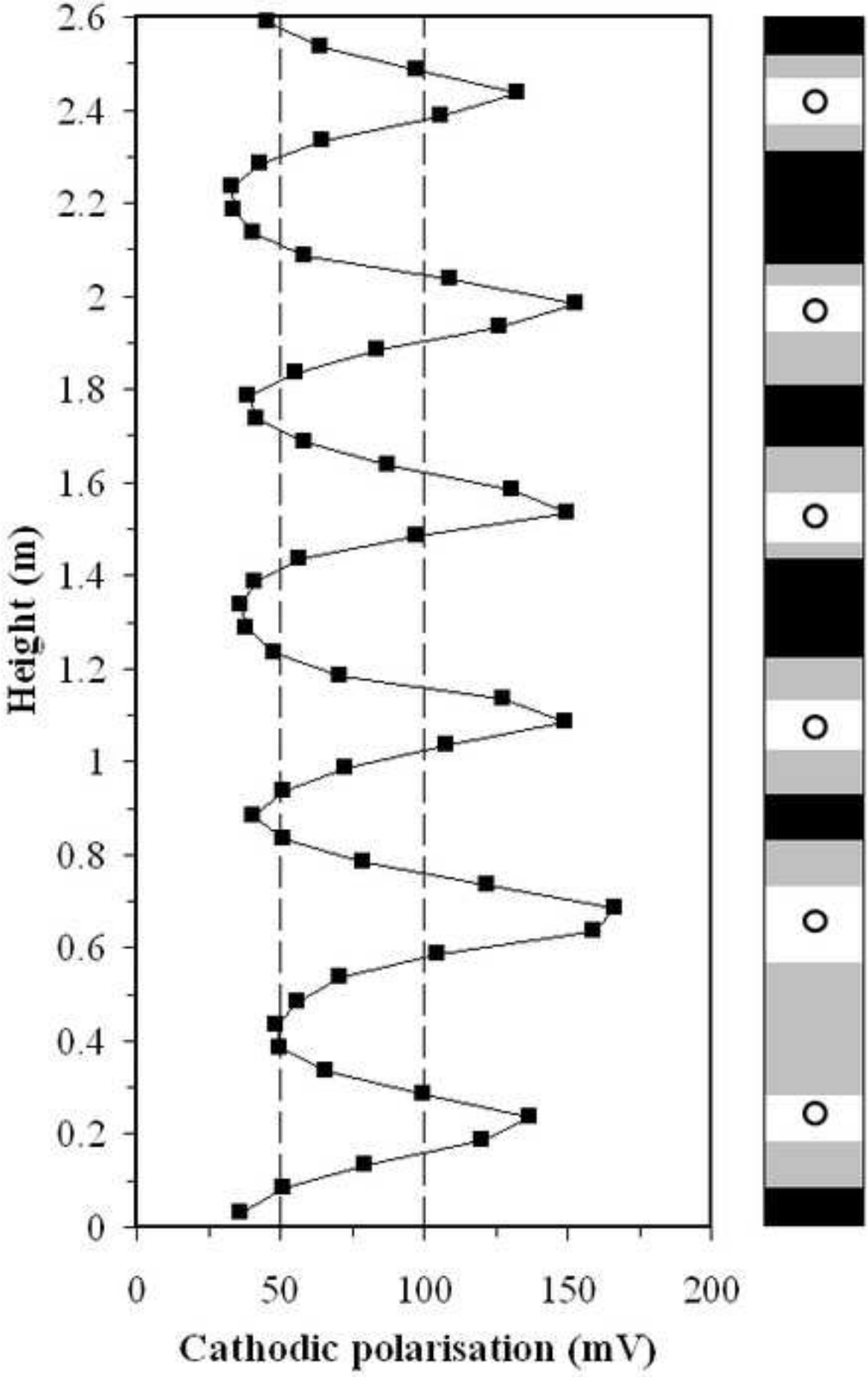

Figure-12
Click here to download high resolution image

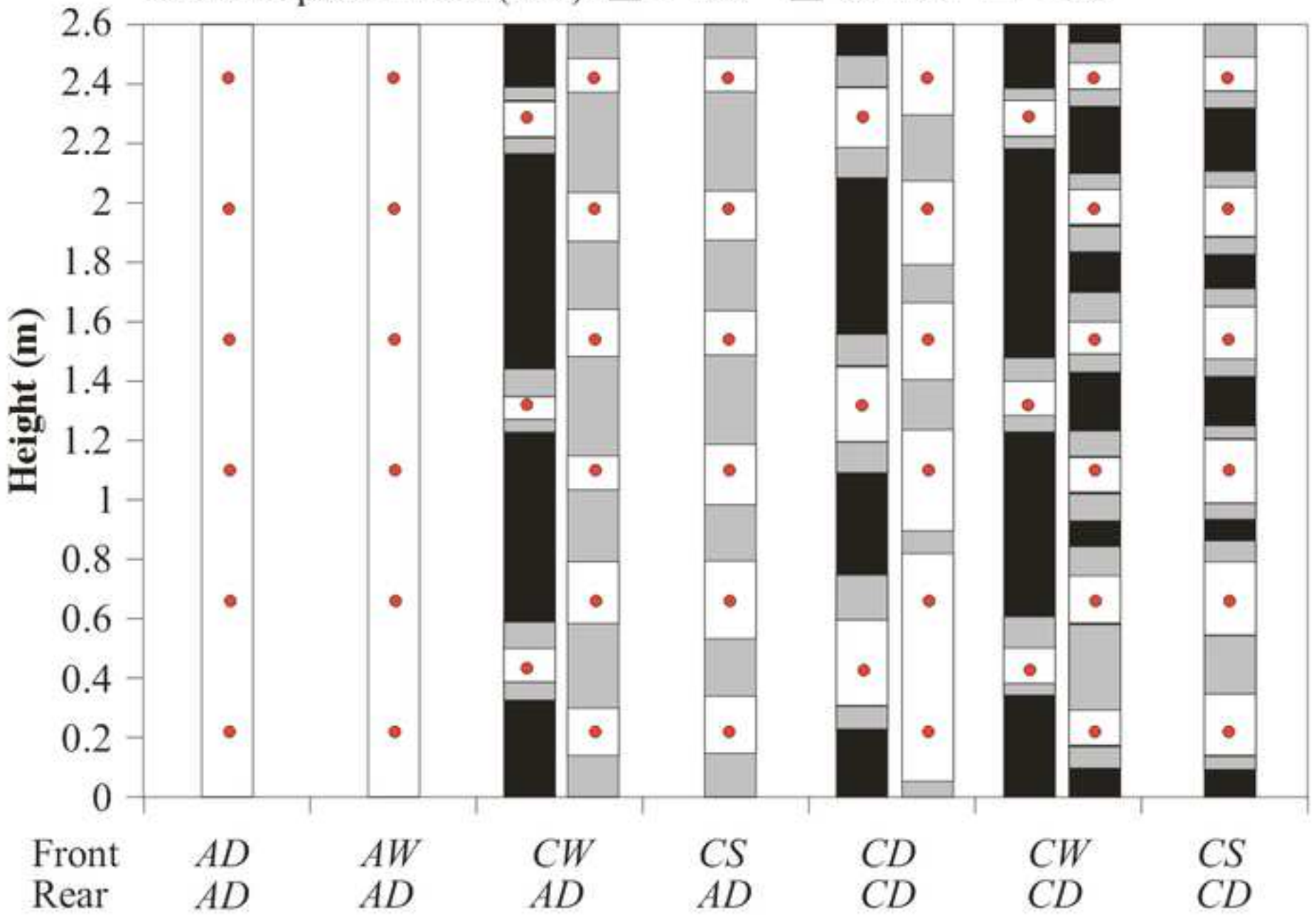

Figure-13
Click here to download high resolution image